LASERS AND AMPLIFIERS

PACS numbers: 42.55.Lt; 42.60.Lh; 33.20.Wr
DOI: 10.1070/QE2001v031n05ABEH001965

The role of optical transitions between ionic and Rydberg states in a KrF laser

V V Datsyuk

***Abstract*. The upper laser level of a KrF laser is treated as a cluster containing several hundreds vibration–rotation energy levels of the electronic state *B*, which is mixed due to collisions with the close ionic state *C*. The KrF (*C*) state is depleted as a result of optical transitions to a higher Rydberg state. This model explains the experimental data on the picosecond dynamics of the light amplification. The possibility of using a KrF laser as an amplifier of radiation with a wavelength of 120 nm is discussed.**

Keywords: *KrF laser, molecular kinetics, Rydberg state.*

1. Introduction

The dynamics of the laser gain g in the active medium of a KrF laser after its saturation with short light pulses was studied experimentally more than ten years ago [1 – 4]. It was found that the recovery of g has two stages (slow and fast):

$$g(t) = g_{st} - \Delta g\left[R_f \exp\left(-\frac{t}{\tau_f}\right) + R_s \exp\left(-\frac{t}{\tau_s}\right)\right], \qquad (1)$$

where the time $t \geqslant 0$; g_{st} is the small signal gain for $t < 0$; $R_f + R_s = 1$; $\Delta g = g_{st} - g(0)$, the subscripts f and s correspond to the fast and slow stages of recovery. Fast recovery of g in various gas mixtures occured for the time $\tau_f \approx 60$ ps. According to Refs [5, 6], the slow recovery time τ_s is the lifetime of excimer molecules KrF (B, C) $\tau_u \simeq 2$ ns. Similar processes of the recovery of g were also observed for other excimers of inert gas halides like XeCl [2, 7] and XeF [4].

The picosecond dynamics of recovery of the gain of an excimer laser was explained by the following processes: depopulation of the lower laser level, rotational relaxation in the optically active electronic state B, and collisional mixing of the B and C states [7]. Each of these processes provides the value of τ_f to be equal approximately to the time τ_0 of gas-kinetic collisions. Indeed, $\tau_f \simeq \tau_0$, in accordance with Table 1 containing the experimental data on the parameters of fast recovery of g. In experiments [1, 2], the fast recovery coefficient R_f was almost independent of t_p for 0.25 ps $< t_p <$ 5 ps. In experiment [3], similar gas mixtures and the same pump as in Refs [1, 2] (electric discharge) were used with $t_p = 1$ ps. Therefore, the value of R_f must be approximately equal to 0.25. However, the measured value $R_f = 0.1$ turned out to be equal to half this value. This discrepancy was not explained even with the help of complicated KrF laser models [8].

Table 1. Parameters of fast recovery of the gain for a KrF laser.

Buffer gas	Pressure/ bar	t_p/ps	τ_f/ps	R_f	Reference
He	2.3	5	63	0.20	[1]
He	2.3	0.26	54 ± 8	0.25 ± 0.04	[2]
He	2.5	1	67	0.10	[3]
Ne	2.5	1	67	0.10	[3]

Note: t_p is the duration of a saturating light pulse.

In this work, an attempt is made to explain the kinetics of the formation of the upper laser level of a KrF laser on the picosecond time scale. First, we estimate the contribution to R_f from each of the kinetic processes mentioned above. Such an analysis does not allow us to interpret the experimental data [1 – 4]; the theory agrees with the results obtained in Refs [1 – 4] only owing to new experimental data [9]. Namely, we observed in Ref. [9] the change in the spectral dependence of g for a KrF laser amplifier under the conditions when the KrF (B) state was depleted by a saturating light pulse, while the population of the KrF(C) state remained high. On the basis of these and other experimental data, absorption bands in the gain spectrum of the KrF laser were identified.

According to Ref. [9], the narrow-band absorption with a peak at 248.91 nm is related to a transition from the ground KrF(C) vibrational level to the Rydberg state $^2\Pi$ (most likely, the $F^2\Pi$ state; see Fig. 1). Broadband absorption at 247.6 nm is related to a transition from the KrF(B) state to the bound Rydberg KrF($E^2\Sigma$) state. The analysis of the picosecond dynamics of the gain of a KrF laser can be treated as an additional argument in favour of the model [9]. The number of KrF excimers transferred from the C state to the F state by a saturating light pulse can be deter-mined by using the data presented in Table 1. It will be shown below that this number is large and comparable with the number of KrF($B \rightarrow X$) phototransitions.

V V Datsyuk Department of Physics, Shevchenko National University, Vladimirskaya ul. 64, 01033 Kyiv, Ukraine

Received 9 November 2000; revision received 19 February 2001
Kvantovaya Elektronika **31** (5) 401 – 406 (2001)
Translated by Ram Wadhwa

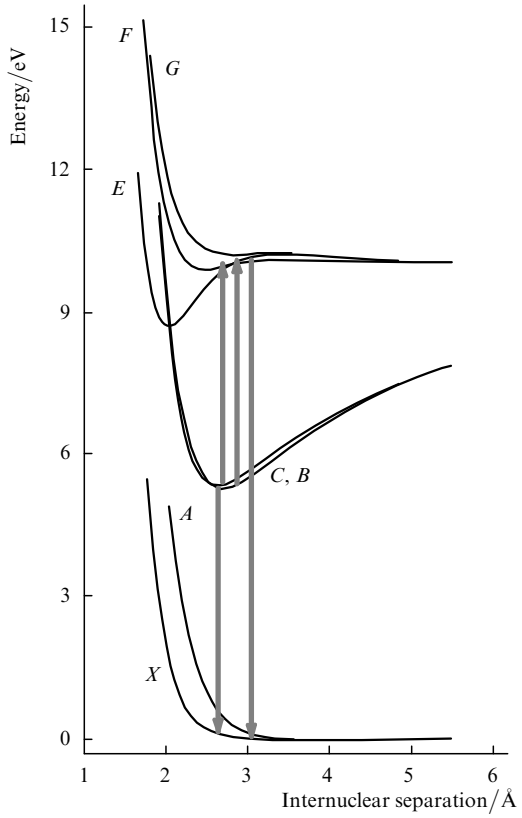

Figure 1. Electronic terms of the KrF excimer [10] and the main optical transitions.

2. Depopulation of the lower laser level

In a KrF excimer laser, the radiative $B \rightarrow X$ transition terminates at the repulsive part of the electronic term KrF(X) [11]. The slopes of the potential curves of the KrF(X) and KrF(B) states are approximately identical in this region of internuclear separations. Therefore, the fly-off time for the KrF(X) molecules formed as a result of the $B \rightarrow X$ transition must not exceed the period of the KrF(B) excimer oscillations, which is equal to 0.1 ps. Indeed, the lifetime of the lower KrF laser level is reported in the literature as 17 fs [8, 12]. Because this is much smaller than t_p, the depopulation of the lower laser level obviously does not affect the picosecond dynamics of the KrF laser.

3. Effect of rotational relaxation

To study the effect of rotational relaxation on g, we consider the dependence of the gain on the rotational distrbution as well as the variation of the rotational distribution upon saturation of the KrF laser by short pulses.

To find the first dependence, we calculated the stimulated emission cross section $\sigma_{v,j}(\lambda)$ for transitions from various rotational levels j of lower vibrational states v of KrF(B) molecules (hereafter, λ is the transition wavelength). The calculations were carried out using the potentials of states B and X and the functions of the dipole moment μ of the $B \rightarrow X$ transition from Ref. [11]. The maximum value $\mu = 2.8$ D was taken from Ref. [13]. The functions $\sigma_{v,j}(\lambda)$ obtained in this way were used to determine the effective stimulated emission cross section:

$$\sigma_{\text{eff}}(\lambda) = \sum_{v=0}^{4} \sigma_v(\lambda) n_v \Big/ \sum_{v=0}^{4} n_v, \quad \sigma_v(\lambda) = \sum_j p_j \sigma_{v,j}(\lambda). \quad (2)$$

Here, σ_v is the stimulated emission cross section for a transition from the vibrational level v with the population n_v; p_j is the population of the rotational level.

Calculations were made for different rotational distributions for the same vibrational distribution. The vibrational distribution was described by the analytic expression [14]:

$$n_v = a\mathscr{F}\left(\kappa, 1; \frac{\varepsilon_v}{T}\right) \exp\left(-\frac{\varepsilon_v}{T}\right), \quad (3)$$

where a is a constant; $\mathscr{F}$ is the degenerate hypergeometric function of the first kind; ε_v is the vibrational energy; T is the gas temperature in energy units; $\kappa \equiv \tau_v/\tau_u$; τ_v is the vibrational relaxation time; the characteristic value $\kappa = 0.3$ used here corresponds to the vibrational temperature $T_v = T/(1-\kappa) \simeq 430$ K. The Boltzmann population of 150 rotational levels was taken into account in the calculations made for different rotational temperatures T_r. It follows from Fig. 2 that a considerable increase in the value of T_r from 300 to 900 K results in a decrease in the σ_{eff} maximum by only 8 %. Fig. 2 also shows that the dependence of $\sigma_{\text{eff}}(\lambda)$ on the vibrational temperature is also weak. Thus, the rotational distribution in each vibrational state KrF(B) does not affect the gain

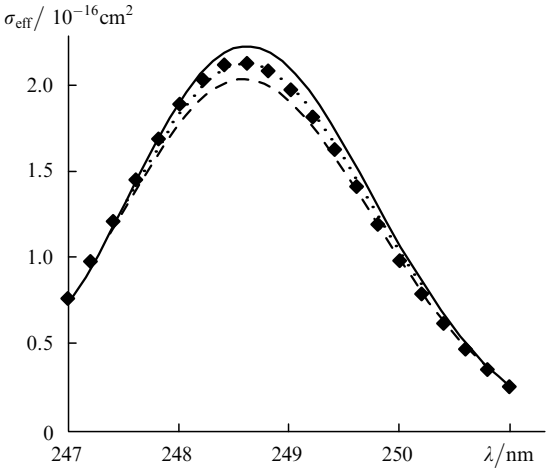

Figure 2. Dependences of the effective stimulated emission cross section on the wavelength calculated for the vibrational temperature $T_v = 430$ K and rotational temperature $T_r = 300$ K (solid curve), 600 K (dotted curve) and 900 K (dashed curve). The same dependence for $T_v = 500$ K, and $T_r = 300$ K is shown by squares.

$$g(\lambda) = \sigma_{\text{eff}}(\lambda) \sum_{v=0}^{4} n_v.$$

Let us now compare the rates of variation of n_0 and $\langle\varepsilon\rangle$, where

$$\langle\varepsilon\rangle = \frac{1}{n_0} \sum_j \varepsilon_{0,j} P_{0,j}$$

is the mean rotational energy of KrF(B, $v = 0$) excimers; $\varepsilon_{v,j}$ and $P_{v,j}$ are the energy and population of the vibration–rotation level KrF(B, v, j), respectively. During the

propagation of a light pulse, the population $P_{v,j}$ decreases according to the law

$$\frac{dP_{v,j}}{dt} = -c\int \sigma_{v,j}(\lambda)\rho(\lambda)d\lambda P_{v,j},$$

where c is the velocity of light, and $\rho(\lambda)\,d\lambda$ is the density of photons with a wavelength lying in the interval between λ and $\lambda + d\lambda$. The rates of variation of n_0 and $\langle\varepsilon\rangle$ depend on $\rho(\lambda)$ and are described by the following equations:

$$\frac{1}{n_0}\frac{dn_0}{dt} = -c\int \sigma_0(\lambda)\rho(\lambda)d\lambda, \qquad (4)$$

$$\frac{1}{\langle\varepsilon\rangle}\frac{d\langle\varepsilon\rangle}{dt} = -\frac{1}{n_0}\frac{dn_0}{dt} - \frac{c\sum_j\int \sigma_{0,j}(\lambda)\rho(\lambda)d\lambda\,\varepsilon_{0,j}P_{0,j}}{\sum_j \varepsilon_{0,j}P_{0,j}}.$$

For simplicity, the right-hand sides of these equations were calculated for $t = 0$, using the Gaussian distribution

$$\rho(\lambda) = \rho_0 \exp\left[-4\ln 2\left(\frac{\lambda-\lambda_0}{\Delta\lambda}\right)^2\right] \qquad (5)$$

for $\lambda_0 = 248.5$ nm [1] and the emission line width $\Delta\lambda \leqslant 1$ nm. These values of the parameters led to the expression

$$\frac{1}{\langle\varepsilon\rangle}\frac{d\langle\varepsilon\rangle}{dt} \simeq -0.035\,\frac{1}{n_0}\frac{dn_0}{dt}.$$

It follows from this relation that the variation in the rotational temperature $T_r = \langle\varepsilon\rangle$ can be neglected. Indeed, a variation in the value of n_0 by a factor of e increases the rotational temperature of the KrF(B, $v = 0$) state from 300 K to about 310 K. According to Fig. 2, such an increase in the value of T_r does not affect the stimulated emission cross section. Thus the rotational relaxation in the KrF(B) state does not play a noticeable role in the picosecond dynamics of the gain in a KrF laser.

Because the depopulation of the lower laser level and the rotational relaxation of the KrF(B) state can be neglected, the picosecond dynamics of the gain was attributed to the mixing of KrF(B) and KrF(C) states in collisions with buffer gas atoms [8].

4. Collisional mixing of the KrF(B) and KrF(C) states

Let us denote by θN the total population of the optically active vibration–rotation levels of KrF(B). These states are in thermal equilibrium with the neighbouring vibration–rotation levels of the KrF(C) state having a total population of $(1-\theta)N$. If a part of the excimers is removed from the state B, the collisions of excimers with the buffer gas atoms will lead to the fast population of the KrF(B) state from the reservoir state C. Analysing the balance of population of the KrF(B) and KrF(C) states, we obtain

$$R_f = 1 - \theta. \qquad (6)$$

This relation has a clear physical meaning. In the hypothetical case $\theta \simeq 0$, only an insignificant part of the excimers contributes to the gain. A variation in their population θN does not affect the total population N. Therefore, $R_f \simeq 1$ and $R_s \simeq 0$. In the opposite case $\theta \simeq 1$, the energy is not stored in the dark states, and hence there is no rapid recovery of the gain. Consequently, $R_f \simeq 0$ and $R_s \simeq 1$.

In a KrF laser, hundreds of vibration–rotation levels of the KrF(B) state with energies lying in an interval of the order of 10^3 cm^{-1} contribute to the stimulated emission of light. This statement is illustrated in Fig. 3 showing the dependences $\sigma_v(\lambda)$ corresponding to various vibrational energies of the KrF(B) state from $\varepsilon_{0,0} = 165$ cm^{-1} to $\varepsilon_{3,0} = 1140$ cm^{-1} (the vibrational quantum of the KrF(B) state is $\hbar\omega_B = 330$ cm^{-1} [11]). The rotational energies of states contributing to $\sigma_{eff}(\lambda)$ are also spread over a wide interval. For example, the rotational level KrF(B, $v = 0$) with $j = 63$ and having a population of 10 % of the maximum value at $T_r = 300$ K has $\varepsilon_{0,63} = 962$ cm^{-1}.

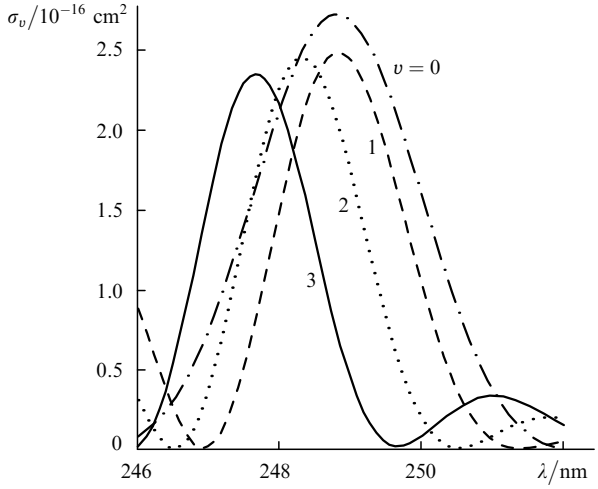

Figure 3. Stimulated emission cross sections calculated for transitions from various vibrational KrF(B) levels.

Obviously, the population of a large number of optically active vibration–rotation levels of the KrF(B) state must be equal to about half the total population of the energy levels in a cluster of collisionally mixed KrF(B, C) states. In other words, the approximate equality $\theta \simeq 0.5$ should be satisfied. Approximating the excimer distribution over the lower vibrational levels by a Boltzmann function with the vibrational temperature T_v [14], we arrive at a more exact expression for θ:

$$\theta = \left[1 + \frac{\sinh(\hbar\omega_B/2T_v)}{\sinh(\hbar\omega_C/2T_v)}\exp\frac{T_{eB} - T_{eC}}{T_v}\right]^{-1}, \qquad (7)$$

where $T_{eB} - T_{eC} \equiv \Delta T_e$ is the difference between the minima of the potentials of states B and C. In computer models of a KrF laser [15, 16], a positive value of $\Delta T_e = 80$ cm^{-1} was taken from Ref. [17].

The predicted value of $R_f \simeq 0.5$ obtained from expressions (6) and (7) is much higher than the experimental values of R_f [1–4]. In principle, one of the experimental values ($R_f = 0.25$ or 0.10) can be attributed to an incorrect value of ΔT_e given in the literature. In this case, the equality

$$\Delta T_e = T_v \ln\frac{R_f}{1 - R_f}$$

leads to a new negative value of ΔT_e. Thus, $\Delta T_e = -T_v \times \ln 3 \simeq -380\ \mathrm{cm}^{-1}$ for $R_f = 0.25$ and a characteristic value of $T_v = 500$ K. Even if we assume such a large error in the generally accepted value of ΔT_e, the spread of R_f over a wide interval 0.10–0.25 is hard to explain.

5. Radiative transitions between the KrF(B) state and the Rydberg state KrF(E)

In order to explain the experimental values of R_f, we should consider the radiative transitions from states B and C to the higher Rydberg states. Two types of radiative transitions must exist for a KrF molecule [9]: KrF(B) $\rightarrow$ KrF($E\ ^2\Sigma$) and KrF(C) $\rightarrow$ KrF($F\ ^2\Pi$). To simplify the analysis, we consider the effect of these transitions on R_f independently.

Let us first study the role of broadband absorption of light transferring the KrF excimers from the B state to higher vibrational levels ($v \geqslant 20$) of the Rydberg state E. For simplicity, we assume that the depopulation of these levels as a result of vibrational relaxation and dissociation occurs with times of the order of τ_0. In this case, we obtain from the balance equations for the populations of the KrF(B), KrF(C) and KrF(E) states

$$R_f = \frac{1}{2}\frac{\gamma_B - 3}{\gamma_B - 2}, \tag{8}$$

where $\gamma_B \equiv \sigma_{BX}/\sigma_{EB}$; σ_{BX} and σ_{EB} are the stimulated emission cross sections for the KrF($B \rightarrow X$) and KrF($E \rightarrow B$) transitions, respectively. Formula (8) gives $R_f < 0.5$, but the value $R_f \simeq 0.25$ will be obtained if $\sigma_{BE} \simeq \sigma_{BX}/4$. For such a strong absorption of light at the $B \rightarrow E$ transition, which is accompanied by a fast depopulation of the KrF(E) state, lasing in a KrF laser would be apparently impossible. In our view, it can be assumed that $\gamma_B \geqslant 10$. In this case, the deviation of R_f from 0.5 can be disregarded. Assuming that the depopulation of the KrF(E) levels is a slow process, we obtain $R_f > 0.5$.

Thus, in spite of its significance, the self-absorption of light by the B state considered above does not explain the measured values of R_f. The only process that has not been considered so far is the KrF($C \rightarrow F$) transition.

6. Radiative transitions between the KrF(C) state and the Rydberg state KrF(F)

According to Ref. [9], a transition occurs between the C state and the Rydberg state KrF($^2\Pi$) correlating with the pair Kr*(^3P) – F(^2P):

$$\mathrm{KrF}(C) + \frac{hc}{\lambda} \rightarrow \mathrm{KrF}(^2\Pi) \rightarrow \mathrm{Kr}^*(^3P) + \mathrm{F}(^2P). \tag{9}$$

This transition is responsible for the dip in the gain spectrum of a KrF laser at 248.91 nm. According to the Gaussian model used in Ref. [18] for simulation of spectra, the absorbtion coefficient dependens on λ in nanometers) as

$$\alpha_C(\lambda) = 0.32 g_0 \exp\left[-4\ln 2\left(\frac{\lambda - 248.91}{0.27}\right)^2\right], \tag{10}$$

where g_0 is the gain at $\lambda_0 = 248.4$ nm. A more complex dependence $\alpha_C(\lambda)$ can be obtained by using the electronic potential of the repulsive Rydberg state from [18]

$$U = 80949 + 3 \times 10^5 \exp(-3.857r) + 2 \times 10^{15} \exp(-16.657r), \tag{11}$$

where U is taken in inverse centimetres, and r is the internuclear separation in angstroms. The results of calculations are presented in Fig. 4. Calculations were made by taking into account the transitions from 101 rotational levels of five KrF(C) vibrational states. The rotational distribution was assumed to be the Boltzmann distribution with the gas temperature T. The population of vibrational states was estimated by formula (3) for $\kappa = 0.3$.

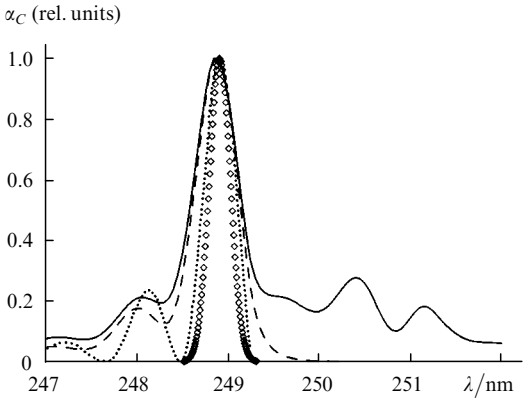

Figure 4. Absorption spectrum related to the KrF*($C, v = 0-4$) $\rightarrow$ Kr* + F transition (solid curve). The dashed and the dotted curves correspond to the contributions from the ground vibrational state KrF($C, v = 0$) and the ground rotational state KrF($C, v = 0, j = 0$), while the circles show the absorption spectrum $\alpha_C(\lambda)$ described by Eqn (10).

Calculations show that the spectral profile of $\alpha_C(\lambda)$ varies strongly with κ for $\lambda \geqslant 250$ nm. However, in the KrF($B \rightarrow X$) emission region of the laser investigated by us, the smooth function $\alpha_C(\lambda)$ depends weakly on κ. In this spectral region, the absorption of light is caused by transitions from the KrF($C, v = 0$) vibrational state. If a large number of rotational levels of the state KrF($C, v = 0$) is taken into account, the function $\alpha_C(\lambda)$ is found to be much broader than function (10). For our analysis, however, the important fact is that a comparatively strong absorption of light exists for 248 nm $< \lambda <$ 249 nm if we take into account only one transition from the zeroth rotational level of KrF($C, v = 0$).

The absorption of light competes with the gain characterised by the function

$$g(\lambda) = g_0 \exp\left[-4\ln 2\left(\frac{\lambda - 248.4}{2.3}\right)^2\right]. \tag{12}$$

The role of transition (9) in molecular kinetics depends on its contribution to the ratio γ of the gain to the total absorption coefficient

$$\gamma = \left(\gamma_m^{-1} + \gamma_C^{-1}\right)^{-1}, \quad \gamma_C \equiv \frac{\int g\rho \mathrm{d}\lambda}{\int \alpha_C \rho \mathrm{d}\lambda},$$

where γ_m is the ratio of the gain to the broadband absorption coefficient of the medium [15, 19]. The ratio γ_m is determined by the active medium components F_2, F^-, Kr_2^+

Kr_2F^*, Ar_2^+, Ar^{**}, and Kr^{**}. According to the experimental data, the value of γ for a KrF laser lies between 10 and 30, the higher values corresponding to electric-discharge-pumped lasers, and the lower ones to the electron-beam-pumped lasers [18, 20].

It is well known that the absorption of light in a laser amplifier leads to the saturation of the light pulse power ($\partial\rho/\partial x \simeq 0$). Because the power of a saturated pulse does not change during its propagation in the active medium, the energy of optically active molecules is transformed into the energy of light absorption products rather than into the light energy.

Consider two opposite cases. At first, we assume that

$$\gamma_C \ll \gamma_m. \tag{13}$$

In this case, the absorption in the active medium takes place mainly due to transition (9). During the propagation of a saturating light pulse, the number of the $KrF(B) \rightarrow Kr + F(^2P)$ transitions will be approximately equal to the number of $KrF(C) \rightarrow Kr^*(^3P) + F(^2P)$ transitions. Consequently, the fast light recovery factor is $R_f \simeq 0$, which is close to the experimental value $R_f = 0.10$ [3].

In the opposite case of $\gamma_C \gg \gamma_m$, the value of γ does not depend on absorption (9), and hence a decrease in the population of the C state during propagation of a light pulse can be neglected. In this case, $R_f \approx 0.5$.

Unfortunately, the exact value of γ_C cannot be determined from the data available in the literature. For example, the values of γ_C obtained by two different methods are compared in Fig. 5. In both cases, the spectral density of photons of the saturating pulse was approximated by Gaussian function (5) with $\lambda_0 = 248.5$ nm. In one case, $\gamma_C(\Delta\lambda)$ was calculated with the help of Eqn (10), while in the other case this dependence was found using the Rydberg state potential (11). For $\Delta\lambda = 0.1$ nm, which corresponds to $t_p = 1$ ps, these two methods of calculation gave $\gamma_C = 916$ and 8.6 respectively.

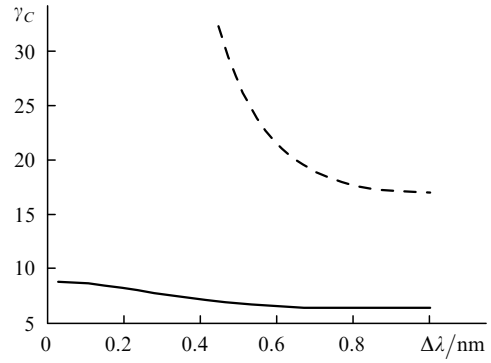

Figure 5. Parameter γ_C calculated for the function $\alpha_C(\lambda)$ described by Eqn (10) (dashed curve) and by the solid curve in Fig. 4 (solid curve) using the Gaussian spectral distribution (5) with $\lambda_0 = 248.5$ nm for the saturating light pulse.

Apparently, the real value of $\gamma_C \approx 30$, and $\gamma_C \simeq \gamma_m$ for electric-discharge lasers. First, the decrease ΔN_C in the population of the C state for such a ratio will be equal to about half the decrease ΔN_B in the population of the B state. Therefore, $R_f \approx 0.25$ for electric-discharge KrF lasers. Second, the dependence of γ_m on the composition of the active medium can explain, along with the dependence of γ_C on λ_0 and $\Delta\lambda$, the variation in the experimental values of R_f over a wide range 0.10 – 0.25. Third, the value of $\Delta N_C \Delta N_B^{-1}$ in an electron-beam-pumped KrF laser should be considerably lower than unity due to lower values of γ_m, hence $R_f \approx 0.5$ in such a laser. The latter statement is consistent with the results of our recent investigations [9] explaining the picosecond dynamics of the spectrum of a KrF electron-beam amplifier.

Thus, the absorption of light by $KrF(C)$ molecules makes it possible to explain all the experimental results available for R_f, and to predict new effects. Note the effect that should be observed for a saturating light pulse with $\lambda_0 = 248.9$ nm. In this case, $\gamma_C \ll 10$ for $\Delta\lambda \leqslant 1$ nm, and inequality (13) is valid. Therefore, the number of photons of wavelength λ_0 emitted during the propagation of a saturating pulse will be approximately equal to the number of $KrF(F)$ excimers formed. In principle, the entire population of the ground vibrational $KrF(C)$ level can be transferred to a Rydberg state.

The transfer of a considerable fraction of the population of the upper laser level of a $KrF(B \rightarrow X)$ laser to the Rydberg states is interesting from the point of view of the gain in the region of $\lambda \simeq 120$ nm. Indeed, because of the low symmetry of the electronic states of KrF, all optical transitions $KrF(B \rightarrow X)$, $KrF(E \rightarrow B)$, and $KrF(E \rightarrow X)$ are allowed (see Fig. 1) and have comparable dipole moments [10]. Unfortunately, no experimental verification of the theoretical results obtained in [10] has been reported in the literature so far. However, the data published in 1977 are sufficient for estimating the emission properties of the KrF excimers in the spectral region 120 nm. Thus, we can determine the cross section $\sigma_R \simeq 10^{-26}$ cm^4 W^{-1} for anti-Stokes scattering of light [21] for a Raman transition between the states B, E and X with $\lambda \simeq 120$ nm. Because of the high spectral density of individual electronic vibration–rotation lines of the $KrF(E \rightarrow B)$ and $KrF(E \rightarrow X)$ transitions, the cross section σ_R should not decrease with decreasing the pump-pulse duration to nanoseconds. This peculiarity raises the hopes of experimental observation of the predicted short-wavelength radiation in a laser amplifier of short pulses.

Finally, note that the radiative transition from the $KrF(C)$ state to the $KrF(F\,^2\Pi)$ state does not result in complete loss of the electronic excitation energy. The $KrF(F\,^2\Pi)$ excimers decay rapidly into pairs $Kr^*(^3P)$–$F(^2P)$, leading to the formation of $KrF(B, C)$ excimers at high vibrational levels [19] as a result of the harpoon reaction of Kr^* with F_2 or the recombination reaction of $Kr^*(^3P)$ and $F(^2P)$. This is followed by a comparatively slow vibrational relaxation of the $KrF(B, C)$ molecules formed in these reactions, which results in the population of the upper laser level.

7. Conclusions

Thus, the analysis of the fast recovery of the gain in a $KrF(B \rightarrow X)$ laser based on new theoretical concepts explains the observed kinetics of population of the upper laser level. Two kinetic processes are of prime importance in this case. The first process is the mixing of the B and C states in collisions of excimers with the buffer gas atoms. This process equalises the populations of the B and C states, and its characteristic time depends on the gas-kinetic

collisions. The second process is an optical transition from the KrF(C) state to a higher Rydberg state. On the one hand, the absorption of light by KrF(C) molecules, which accompanies the stimulated emission at the KrF($B \rightarrow X$) transition, affects the gain spectrum of the KrF laser. The sharp absorption peak at $\lambda = 248.9$ nm makes the gain spectrum narrower, while the broadband absorption in the region 248.4 nm leads to a decrease in the ratio of the gain to the absorption coefficient. On the other hand, the KrF(C) $\rightarrow$ KrF(F) optical transition in electric-discharge KrF lasers transfers a significant part of excimers from the C state to a repulsive Rydberg state.

References

1. Szatmári S, Schäfer F P *Appl. Phys B* **33** 219 (1984)
2. Szatmári S, Schäfer F P *J. Opt. Soc. Am. B* **4** 1943 (1987)
3. Taylor A J, Gibson R B, Roberts J P *Appl. Phys. Lett.* **52** 773 (1988)
4. Szatmári S *Top. Appl. Phys.* **70** 129 (1992)
5. Datsyuk V V *J. Phys. Studies* **4** 37 (2000)
6. Datsyuk V V, Izmailov I A *J. Phys. Studies* **4** 274 (2000)
7. Corcum P B, Taylor R S *IEEE J. Quantum Electron.* **18** 1962 (1982)
8. Kannari F *J. Appl. Phys.* **67** 3954 (1990)
9. Datsyuk V V, Hooker C J, Divall E J, et al. *J. Chem. Phys.* **112** 3766 (2000)
10. Hay P J, Dunning T H, Jr. *J. Chem. Phys.* **66** 1306 (1977)
11. Lo G, Setser D W *J. Chem. Phys.* **100** 5432 (1994)
12. Milonni P W, Gibson R B, Taylor A J *J. Opt. Soc. Am. B* **5** 1360 (1988)
13. Kvaran A, Shaw M J, Simons J P *Appl. Phys B* **46** 95 (1988)
14. Datsyuk V V, Izmailov I A, Kochelap V A *Usp. Fiz. Nauk* **168** 439 (1998)
15. Kannari F, Obara M, Fujioka T *J. Appl. Phys.* **57** 4309 (1985)
16. Lee Y W, Endoh A *Appl. Phys B* **52** 245 (1991)
17. Julienne P S, Krauss M *Appl. Phys. Lett.* **35** 55 (1979)
18. Shaw M J, Divall E J, Hirst G J, et al. *J. Chem. Phys.* **105** 1815 (1996)
19. McDaniel E, Nighan W (Eds.) *Gas Lasers* (New York: Academic Press (1982), Ch. 10
20. Barr J R M, Everall N J, Hooker C J, et al. *Opt. Commun.* **66** 127 (1988)
21. Datsyuk V V *Chem. Phys. Lett.* **329** 477 (2000)